THE ASTROPHYSICAL JOURNAL, 310:937–952, 1986 November 15

COMETARY GRAIN SCATTERING VERSUS WAVELENGTH, OR, "WHAT COLOR IS COMET DUST?"

DAVID JEWITT[1] AND KAREN J. MEECH[1]
Department of Earth, Atmospheric, and Planetary Sciences, Massachusetts Institute of Technology
Received 1986 February 27; accepted 1986 May 2

ABSTRACT

Optical and near-infrared observations of comets are combined in a systematic study of the wavelength dependence of the scattering from cometary grains. At optical wavelengths ($0.35 < \lambda < 0.65$ μm), the grain continua are red compared to the solar continuum. Reduced reddening is observed in the near-infrared ($1.2 < \lambda < 1.6$ μm), both in observations at a spectral resolution $\lambda/\Delta\lambda \approx 30$ and in broad-band photometry. The scattered continuum is neutral near $\lambda \approx 2$ μm, and probably blue at longer wavelengths. This systematic trend in the color of the scattered light with increasing wavelength may be interpreted as evidence that the optically dominant grain size in comets is $a \geq 1$–2 μm. Models of the scattering from various size distributions of grains suggest an important difference between the sizes of the cometary and interstellar grains; the optically important cometary grains are about an order of magnitude larger than the optically important interstellar grains. Submicron grains *are* present in comets, but not in sufficient numbers as to dominate the optical scattering cross section of the grains as a whole. Cometary grains may have grown by agglomeration of pristine interstellar grains in the collapsing cloud from which the comets formed. Variations among the continuum colors of the comets at a given wavelength are highly significant and do not appear to be correlated with heliocentric distance, phase angle, or mass-loss rate. Instead, the color differences appear to result from intrinsic, possibly primordial, differences among the grains in different comets.

Subject headings: comets — spectrophotometry

I. INTRODUCTION

The physical and optical properties of cometary dust grains are of interest for at least two reasons. First, these grains are responsible for much of the light scattered from cometary comae; hence grain optics influence the basic appearances of comets. Second, the grains may be unprocessed (unheated) relics from the time of the formation of the solar system (or before). As such, they may carry information concerning the conditions of formation of comets and planets and may even yield information concerning the interstellar grains (from which they are presumed to be derived).

So far, the most revealing measurements of cometary grains have been those made in the thermal infrared ($\lambda > 5$ μm). When combined with near-infrared measurements, the thermal data can be used to estimate the grain albedo and the grain cross section, and in some cases even an estimate of the effective grain size is possible. The thermal infrared data also show evidence for a broad emission feature near $\lambda \approx 10$ μm, plausibly attributed to a silicate composition. Measurements of the scattered radiation, by contrast, have generally been less informative. In the optical ($0.3 < \lambda < 1$ μm), few detailed studies have been attempted, since the scattered continuum emission is usually swamped by emission from bright molecular bands. Several of the published optical studies are impossible to interpret, since they were made using inadequate spectral resolution. In the near-infrared ($1 < \lambda < 5$ μm), low detector efficiency and poor spectral resolution combine to reduce the usefulness of the measurements. Additionally, the commonly measured near-infrared colors (e.g., $J-H$, $H-K$) are not by themselves very diagnostic of the physical or chemical properties of the grains (Hanner 1980).

Only recently have attempts been made to study optical grain scattering in many comets using standardized, moderate-resolution optical spectrophotometric methods (Remillard and Jewitt 1985; Newburn and Spinrad 1985). The most general property is a slight reddening of the scattered light with respect to the solar continuum. That is, the scattering efficiency of the grains increases with increasing wavelength. Earlier reports of relatively blue continua, and a few reports of continua which changed color according to the viewing geometry, may result from the use of inadequate spectral resolution and the contamination of "continuum" wavelengths by molecular emission. A brief summary of previous continuum observations is given by A'Hearn (1982).

In the present work, we extend our initial study of the optical continua (Remillard and Jewitt 1985) to a larger sample of comets and increase the range of observed wavelengths, by a factor of 7, into the near-infrared. We use the new observations to address the following questions:

1. What are the basic characteristics of the wavelength dependence of scattering from cometary grains?
2. What constraints may be placed on the physical properties of cometary grains and on the grain size distribution from measurements of the scattered light?
3. How do the optical properties of cometary grains compare with the properties of interstellar grains?
4. Are there significant differences among the scattering properties of different comets? If so, are these differences related to heliocentric distance, viewing geometry, the dynamical age of the comet, or to intrinsic differences in the grains? Might the color differences be used to classify

[1] Visiting Astronomer at the Kitt Peak National Observatory, National Optical Astronomy Observatories, operated by the Association of Universities for Research in Astronomy, Inc., under contract with the National Science Foundation; and at the Infrared Telescope Facility, which is operated by the University of Hawaii under contract from the National Aeronautics and Space Administration.

comets in the same way that color differences are used to categorize asteroids?

II. OBSERVATIONS

a) Optical Observations

Optical observations of nine comets were taken using an intensified image dissector scanner (IIDS) on the 2.1 m telescope at Kitt Peak. The IIDS was placed at the f/7.7 Cassegrain focus, giving a focal plane image scale of 12".3 mm^{-1}. A reflection grating of 300 lines mm^{-1} (grating No. 09) was used in the first order, giving a dispersion of ~3.4 Å per channel and a wavelength range from 3500 to 7000 Å. All observations were taken through a circular diaphragm of 8".4 projected diameter. The instrumental resolution through this diaphragm was measured to be 19 Å full width at half-maximum (FWHM). Sky subtraction with the IIDS was performed using simultaneous observations of the sky projected 100" east-west from the object position. Gas emission bands were noticed at the "sky" positions in some of the comets. In these cases, separate sky observations were taken at positions 0°.5 from the comet. Possible instrumental asymmetries between the object and sky beams were canceled by periodically chopping the comet from one beam to the other.

Observations were obtained on the nights of UT 1985 February 16 and 17. The comets observed were Shoemaker 1984s, Levy-Rudenko 1984t, P/Tsuchinshan 1 1984p, P/Schaumasse 1984m, P/Arend-Rigaux 1984k, P/Gehrels 3 1984l, P/Faye 1984h, P/Wolf-Harrington 1984g, and P/Smirnova-Chernykh 1984 V. The comets were identified using a large-format television guider attached to the IIDS. The identification criteria included both the diffuse appearance of the comets and their motion with respect to field stars. On both nights the seeing and the guiding uncertainties (1".5 FWHM and 1" respectively) were small in comparison with the spectrometer diaphragm. Absolute flux calibration of the spectra was achieved using observations of the stars Feige 34, BD +8°2015, Hiltner 600, Ross 640, EG 247, and Grw +70°5824 at similar air masses (Oke 1974; Stone 1977). Spectra of an internal helium-neon-argon source were taken throughout each night to provide wavelength calibration, and quartz-halogen continuum spectra were taken for use as flat fields.

The subsequent reduction procedure included steps to divide each spectrum by the nightly average flat field and to linearize the wavelength scale. The Kitt Peak mean extinction was applied to all observations. Intercomparison of the standard star spectra showed that the flux calibration was internally consistent to better than 5% in each channel. Systematic differences among the spectra of the standard stars were less than ±6% from 3500 to 6500 Å wavelength (i.e., gradient errors were < ±2% per 1000 Å). Slightly larger systematic effects were occasionally seen from 6500 to 7000 Å, leading us to ignore this wavelength region in the following analysis.

A journal of optical observations is given in Table 1. The flux calibrated spectra are shown in order of increasing heliocentric distance in Figures 1*a*–1*c*. The degree of success of the sky subtraction of the IIDS may be judged from the removal of the night sky line at 5577 Å. Spectra of comets Levy-Rudenko and P/Tsuchinshan 1 were taken on both nights; no important differences were observed, and so we have plotted only the first of the spectra of each comet in Figure 1. The figure shows a range of cometary spectra from emission-band–dominated to continuum-dominated. Some of the emission features are identified in Figure 1*a*.

b) Broad-Band Observations in the Near-Infrared

Broad-band photometry of nine comets (Bowell, P/Wild 2, P/Harrington-Abell, P/Smirnova-Chernykh, P/Taylor, P/Thiele, P/Halley, P/Giacobini-Zinner, and P/Giclas) was taken using the 3 m telescope at the NASA-IRTF on Mauna Kea. The observations were obtained on three separate observing runs in 1982 May, 1984 February, and 1985 November. A liquid nitrogen–cooled InSb detector was used for all observations. The 7".2 diameter photometer diaphragm was chopped 10" east-west at 13 Hz in 1982 May and 1984 February, and 60" north-south at 7 Hz in 1985 November, to allow sky subtraction. Observations were taken through the standard *J*, *H*, and *K* filters (centered at 1.25, 1.65, and 2.20 μm wavelength respectively). A journal of the near-infrared observations is presented in Table 2.

Calibration of the *JHK* photometry was achieved by observing standard stars from the list of Elias *et al.* (1982). Extinction was determined in each filter by observing the standard stars at a range of air masses. The photometry is summarized in Table 3. The photometric uncertainties listed in the table are due to small errors in the positioning of the diaphragm with respect to the center of light of the comet and to extinction uncertainties. The short chop distance used for some observations may cause a small error in the background subtraction, due to coma present in the sky beam. However, the *JHK* magnitudes are individually in error by no more than 0.2

TABLE 1

JOURNAL OF OPTICAL OBSERVATIONS

Midintegration Time (UT)	Comet	Midintegration Air Mass	Integration Time (s)	Sky Position[a]
1985 Feb 16 06:20.....	P/Shoemaker 1984S	1.27	1080	100" east-west
1985 Feb 16 08:31.....	Levy-Rudenko	1.28	1200	2160 south
1985 Feb 16 10:25.....	P/Tsuchinshan 1	1.14	1800	1800 north
1985 Feb 16 12:06.....	P/Schaumasse	1.40	1200	1920 north
1985 Feb 17 03:57.....	P/Arend-Rigaux	1.27	1800	100 east-west
1985 Feb 17 05:53.....	P/Gehrels 3	1.30	1600	100 east-west
1985 Feb 17 07:20.....	P/Faye	1.25	2600	100 east-west
1985 Feb 17 08:30.....	P/Wolf-Harrington	1.67	2000	100 east-west
1985 Feb 17 09:44.....	P/Tsuchinshan 1	1.06	2400	1800 north
1985 Feb 17 11:06.....	Levy-Rudenko	1.45	1200	100 east-west
1985 Feb 17 11:57.....	P/Smirnova-Chernykh	1.64	1200	100 east-west

[a] Position used for sky subtraction, relative to the nucleus.

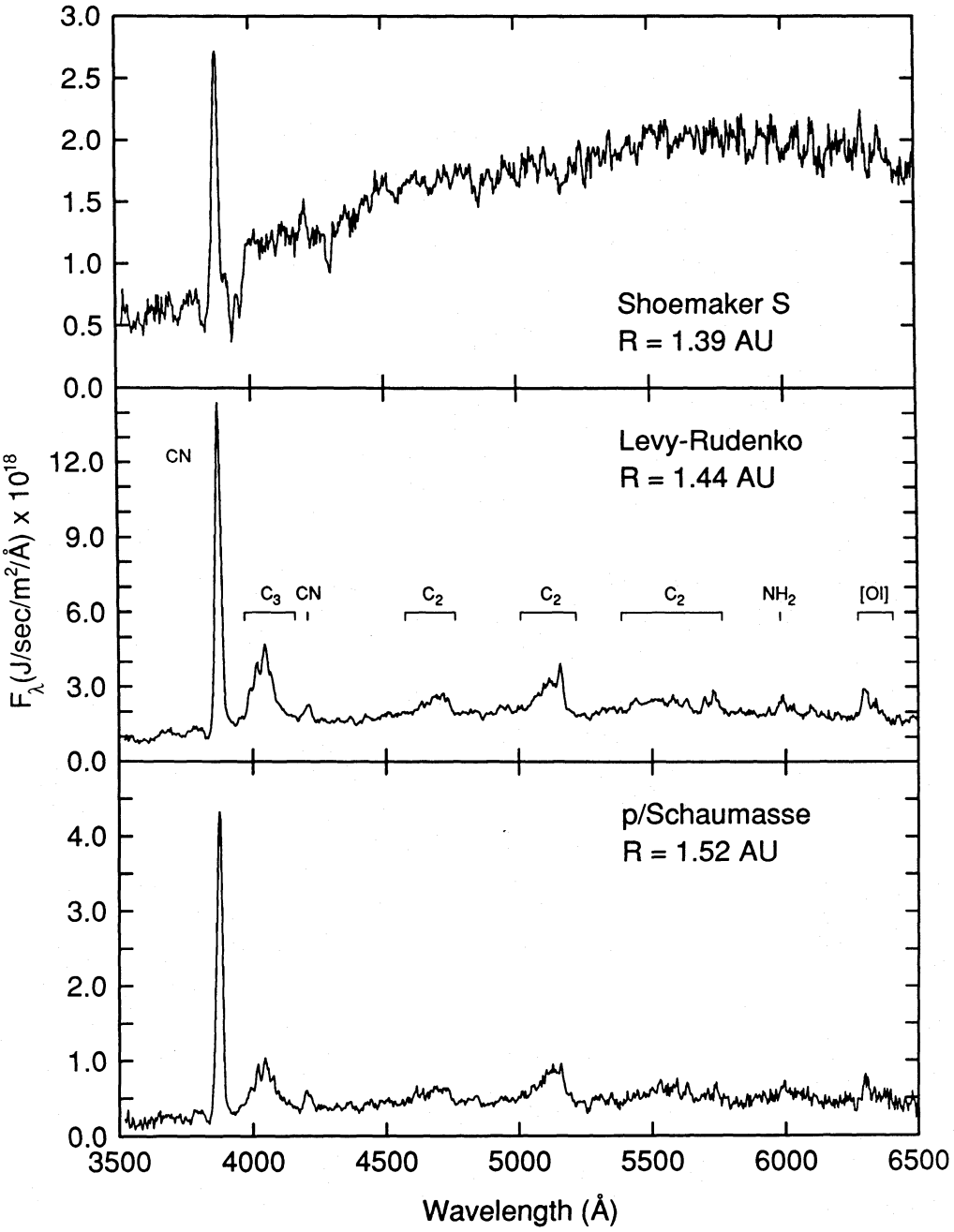

FIG. 1.—Optical spectra of nine comets observed with the IIDS. The sky-subtracted flux density F_λ (W m^{-2} Å^{-1}) within a circular diaphragm of 8″ diameter is plotted vs. wavelength λ (Å) for each comet. No smoothing has been performed on the measured flux densities. Spectra are presented in order of increasing heliocentric distance R.

mag as a result of the imperfect background subtraction, even with the smallest chop distance (10″). The effect on the $J-H$ and $H-K$ magnitude differences is negligible.

c) *Spectral Observations in the Near-Infrared*

Spectral observations of comet P/Wild 2 were taken at the IRTF in 1984 February. The detector and setup were the same as used for the broad-band IR photometry. A circular variable interference filter (CVF) gave a spectral resolution $\lambda/\Delta\lambda \approx 30$ in the range $1.3 < \lambda < 2.4$ μm. The wavelength zero point of the CVF was established through observations of known atmospheric absorption features. Near-infrared flux standards were used to provide absolute calibration of the CVF spectra. The solar analog star 16 Cyg B was also observed. Comet P/Swift-Gehrels was observed on our behalf by G. Neugebauer with the Palomar 5 m telescope and a CVF at a resolution $\lambda/\Delta\lambda \approx 20$ (see Jewitt *et al.* 1982 for details of the observing procedure employed). The comet was observed on UT 1981 November 9 using a 5″ diameter diaphragm.

III. REFLECTIVITIES

The physical quantity of interest is the scattering efficiency of the solid grains, $Q_s(\lambda)$. For practical reasons, however, the spectra are more conveniently described in terms of

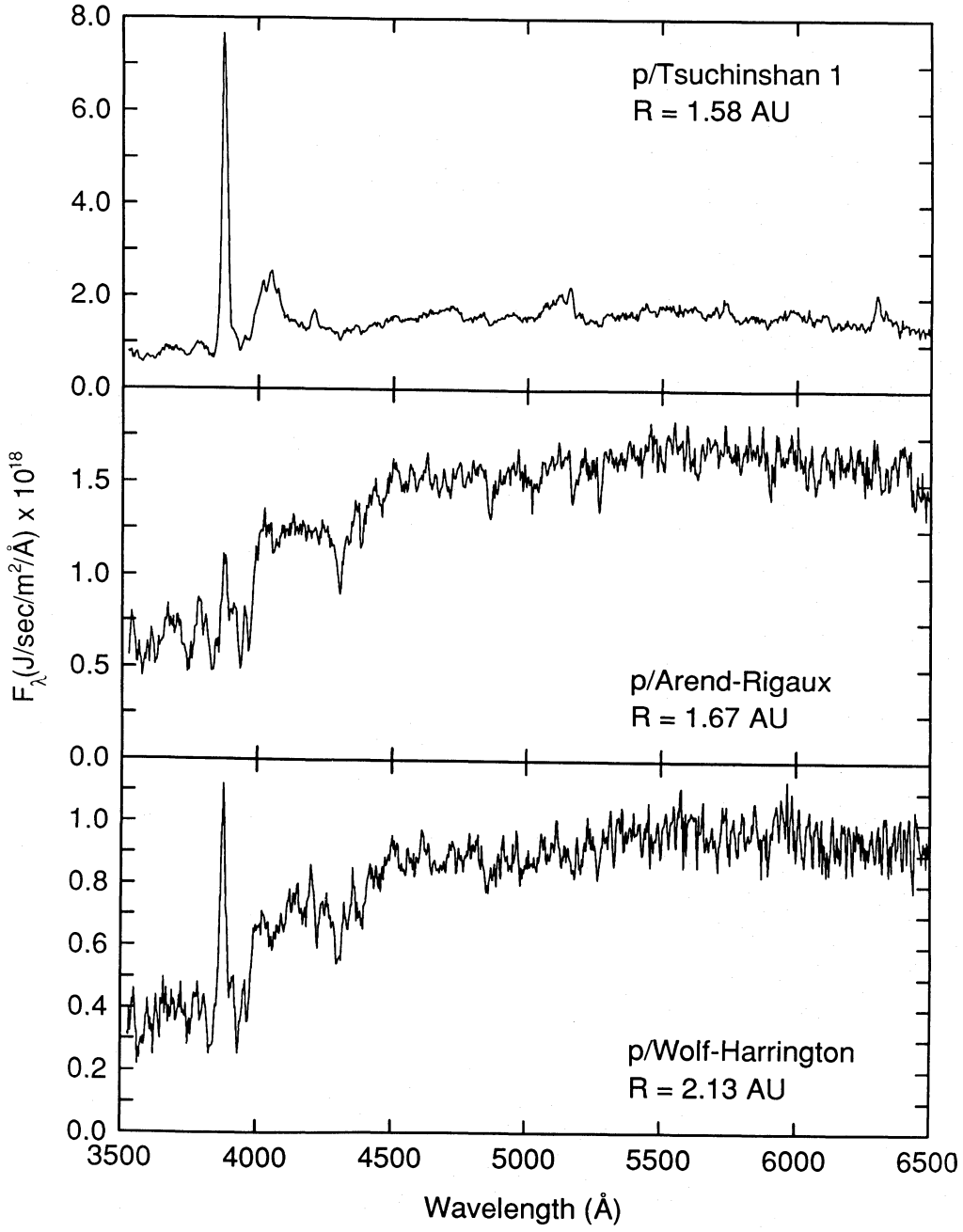

FIG. 1.—*Continued*

"reflectivity," $S(\lambda)$, which is proportional to $Q_s(\lambda)$ provided the coma is optically thin. The optical spectra (Fig. 1) were used to compute the reflectivity, $S(\lambda) = F_\lambda/F_\lambda(\text{Sun})$, at each observed wavelength by dividing the measured flux densities F_λ by the solar spectrum $F_\lambda(\text{Sun})$, as tabulated by Arvesen, Griffin, and Pearson (1969). Before division, the solar spectrum was interpolated to the central wavelength of each IIDS channel and smoothed by a Gaussian of FWHM equal to the instrumental resolution. By inspection, the wavelength intervals 3520–3700, 4390–4450, 5760–5820, 6150–6200, and 6380–6500 Å were determined to be free of molecular bands in each of the comet spectra. The reflectivities within these continuum windows are plotted in Figures 2*a*–2*c*, where they are shown on a common scale to allow easy intercomparison (but note that the scale for P/Gehrels 3 is twice that of the other comets because of the large noise in that faint comet). The plotted reflectivities are normalized to the mean of the reflectivities in the wavelength range $5760 < \lambda < 5820$ Å. Figure 2 shows that the reflectivities of all nine comets increase with increasing wavelength (i.e., the cometary grains are red).

We define the normalized reflectivity gradient between wavelengths λ_1 and λ_2,

$$S'(\lambda_1, \lambda_2) = (dS/d\lambda)/S_{\text{mean}} , \quad (1)$$

in which $dS/d\lambda$ is the rate of change of the reflectivity with respect to wavelength in the interval λ_1 to λ_2, and S_{mean} is the

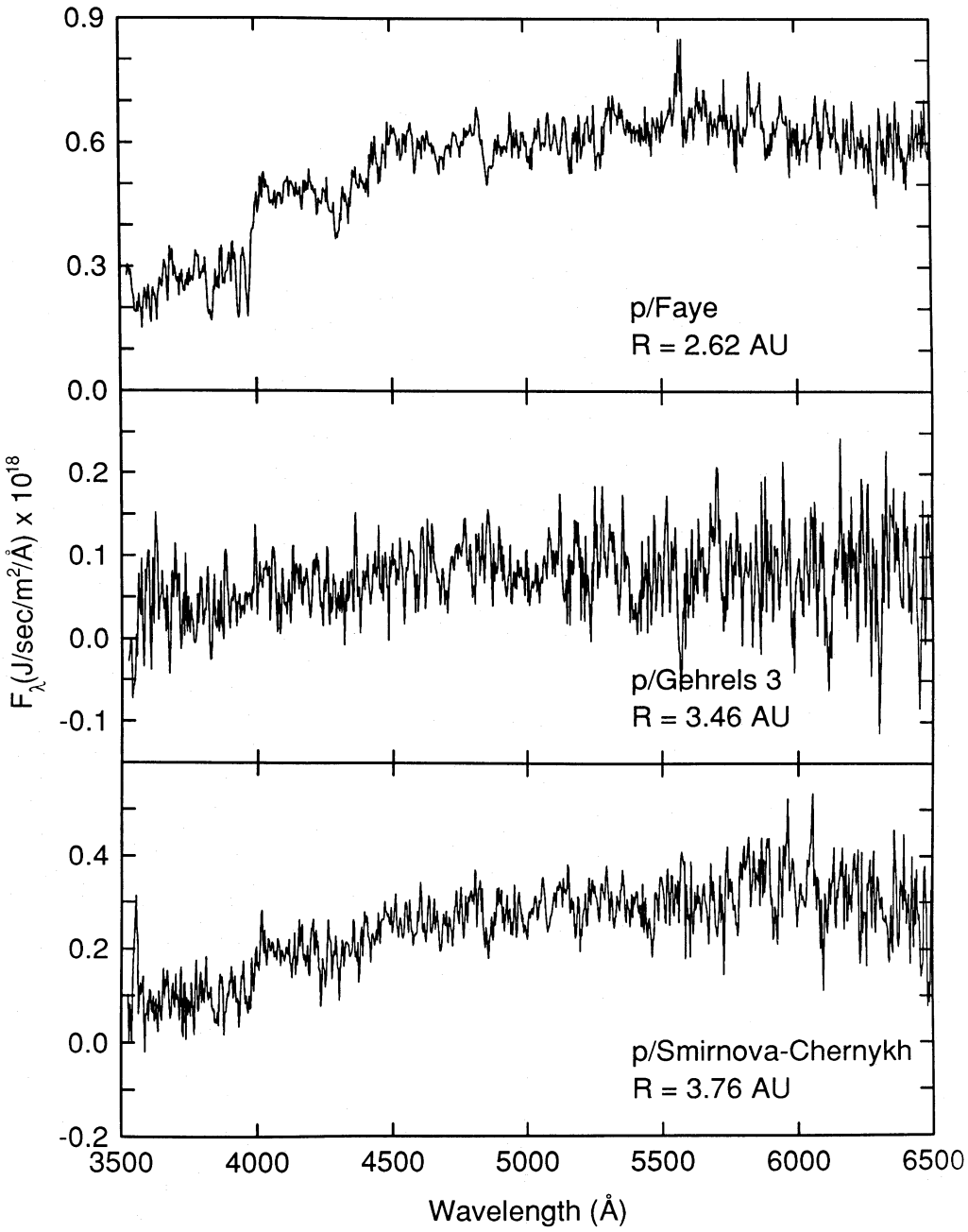

FIG. 1.—*Continued*

mean reflectivity in the observed wavelength range:

$$S_{\text{mean}} = N^{-1} \sum S_i(\lambda) \, . \qquad (2)$$

The $S'(\lambda_1, \lambda_2)$ are expressed in percent per 10^3 Å and provide a convenient measure of the grain color (in fact, we sometimes refer to S' as the "continuum color"). Grain reddening is indicated by $S'(\lambda_1, \lambda_2) > 0$. Values of $S'(\lambda_1, \lambda_2)$ calculated from linear least-squares fits to the optical data are listed in Table 4; the fits are shown in Figure 2. The formal errors of the least-squares fits are small compared with the possible systematic errors ($\pm 2\%$ per 10^3 Å; § II) in all comets except P/Gehrels 3 and P/Smirnova-Chernykh. The latter comets are faint enough that statistical noise is significant. It is pleasing to note that the continuum color of P/Smirnova-Chernykh, $S'(0.35, 0.65) = (16 \pm 3)\%$ per 10^3 Å (Table 4), is similar to the color measured a year earlier with a different instrument by Remillard and Jewitt (1985), namely, $S'(0.37, 0.73) = (16 \pm 1)\%$ per 10^3 Å. The optical normalized reflectivity gradients of the nine comets vary from (5 ± 2) to $(18 \pm 2)\%$ per 10^3 Å.

The normalized reflectivity gradients $S'(\lambda_1, \lambda_2)$ (percent per 10^3 Å) in the $J-H$ and $H-K$ near-infrared wavelength intervals were computed using

$$S'(\lambda_1, \lambda_2) = (20/\Delta\lambda)(10^{0.4\Delta m} - 1)/(10^{0.4\Delta m} + 1) \, , \qquad (3)$$

in which Δm equals the comet color minus the solar color (both in mag), and $\Delta\lambda = \lambda_2 - \lambda_1$, the difference in the effective wave-

TABLE 2

JOURNAL OF NEAR-INFRARED OBSERVATIONS

Midintegration Time (UT)	Comet	Air Mass	Technique[a]
1981 Nov 9 03:20	P/Swift-Gehrels	1.08	CVF
1982 May 29 12:00	Bowell	1.60	*JHK*
1984 Feb 3 06:15	P/Wild 2	1.02	*JHK*
1984 Feb 3 12:45	P/Harrington-Abell	1.02	*JHK*
1984 Feb 3 13:35	P/Smirnova-Chernykh	1.02	*JHK*
1984 Feb 4 06:15	P/Wild 2	1.03	*JHK*
1984 Feb 4 07:00	P/Wild 2	1.10	CVF
1984 Feb 4 09:45	P/Taylor	1.10	*JHK*
1984 Feb 4 11:00	P/Harrington-Abell	1.11	*JHK*
1984 Feb 4 12:05	P/Smirnova-Chernykh	1.08	*JHK*
1985 Nov 12 05:10	P/Theile	1.09	*JHK*
1985 Nov 12 12:05	P/Halley	1.02	*JHK*
1985 Nov 12 14:40	P/Giacobini-Zinner	1.63	*JHK*
1985 Nov 14 14:45	P/Giacobini-Zinner	1.67	*JHK*
1985 Nov 14 14:00	P/Giclas	1.96	*JHK*

[a] *JHK*, broad-band photometry; CVF, circular variable filter spectrum.

lengths of the broad-band *JHK* filter pairs, measured in microns. Equation (3) is the practical equivalent to equation (1), derived under the approximation that the reflectivity is a linear function of λ in the infrared (see the following paragraph for a justification of this approximation). The adopted solar colors are $(J-H)_0 = 0.32$ and $(H-K)_0 = 0.07$ (A'Hearn, Dwek, and Tokunaga 1984). Uncertainties in the solar colors of order 0.1 mag (cf. Johnson *et al.* 1975; Campins, Rieke, and Lebofsky 1985) are comparable to the typical uncertainties of measurement in the near-infrared comet colors and may cause a systematic uncertainty in the reflectivity gradients $\Delta S' \leq 2\%$ per 10^3 Å. The near-infrared $S'(\lambda_1, \lambda_2)$ are listed in columns (8) and (10) of Table 3.

Before proceeding to use the *JHK* photometry to characterize the continuum scattering of cometary grains, we are obliged to present evidence that these broad-band filters give a true measure of the continuum colors and that they are not, for instance, influenced by unresolved absorption or emission features in the near-infrared. This evidence rests largely on the

TABLE 3

BROAD-BAND INFRARED PHOTOMETRY

Comet (1)	R (AU) (2)	Δ (AU) (3)	α (4)	J[a] (5)	$J(1, 1, 0)$ (6)	$J-H$[b] (7)	$S'(J, K)$ (8)	$H-K$[b] (9)	$S'(H, K)$ (10)	Reference (11)
P/Giacobini-Zinner	1.38	0.80	45°	12.26	10.00	0.47	3.5	+0.09	+0.3	1[c]
P/Thiele	1.43	0.58	33	12.35	10.84	0.55	5.3	+0.14	+1.2	1
P/Stephan-Oterma	1.73	0.96	29	12.66	10.35	0.44	2.8	+0.19	+2.0	2
P/Halley	1.76	0.80	10	10.44	9.05	0.45	3.0	+0.14	+1.2	1
P/Giclas	1.87	0.90	7	14.63	13.10	0.41	2.1	...	...	1[d]
P/Harrington-Abell	1.88	0.95	14	15.44	13.56	0.36	0.9	−0.03	−1.7	1[c]
P/Stephan-Oterma	1.98	1.39	28	14.40	11.44	0.54	5.1	+0.17	+1.7	2
P/Taylor	1.98	1.09	17	15.47	13.21	0.55	5.3	+0.09	+0.3	1
P/Kearns-Kwee	2.32	1.63	21	15.54	12.34	0.63	7.1	−0.05	−2.0	2
P/Wild 2	2.40	1.94	23	14.71	11.17	0.45	3.0	+0.19	+2.0	1[c]
P/Gunn	2.77	1.79	6	13.9	10.8	0.41	2.1	+0.16	+1.5	2[c]
P/Gunn	2.94	2.30	17	14.6	10.67	0.5	4.1	+0.25	+3.0	2
Cernis	3.24	3.07	18	12.29	7.80	0.35	0.7	+0.11	+0.7	3[c]
Bowell	3.37	3.55	16	13.44	8.79	0.42	2.3	+0.07	0.0	4
Bowell	3.45	2.51	8	12.26	8.25	0.45	3.0	+0.02	−0.8	1
P/Smirnova-Chernykh	3.56	2.77	11	14.78	10.48	0.43	2.5	+0.16	+1.5	1[c]
Bowell	4.28	3.85	13	13.57	8.43	0.43	2.5	+0.06	−0.2	4
Bowell	4.80	3.85	4	13.65	8.62	0.46	3.2	+0.03	−0.7	4
Elias	5.13	4.31	7	15.3	9.88	0.38	1.4	+0.01	−1.0	2[c]

[a] Typical uncertainty, $\sim \pm 0.05$ to ± 0.1 mag.
[b] Typical color uncertainty, $\sim \pm 0.07$ to ± 0.15 mag.
[c] Average of photometry from more than one night.
[d] Uncertainty, $\sim \pm 0.20$ mag.
REFERENCES.—(1) This work. (2) Hanner *et al.* 1984. (3) Hanner 1984. (4) Hanner and Veeder 1984.

TABLE 4

OPTICAL CONTINUUM SPECTRA

Comet	R (AU)	Δ (AU)	α	$S'(\lambda_1, \lambda_2)$ (per 10^3 Å)	m_{5790}	$m(1, 1, 0)$
P/Shoemaker 1948S	1.39	0.56	36°3	18% ± 2%	15.67	14.14
Levy-Rudenko	1.44	0.64	36.2	5 ± 2	15.67	13.92
P/Schaumasse	1.52	1.18	40.6	10 ± 2	17.29	14.56
P/Tsuchinshan 1	1.58	0.62	13.2	7 ± 2	15.91	14.92
P/Arend-Rigaux	1.67	0.72	13.6	14 ± 2	15.84	14.52
P/Wolf-Harrington	2.13	1.23	14.8	16 ± 2	16.45	13.98
P/Faye	2.62	1.67	8.0	14 ± 2	16.94	13.97
P/Gehrels 3	3.46	2.96	15.2	11 ± 6	19.07	14.60
P/Smirnova-Chernykh	3.76	3.63	15.2	16 ± 3	17.59	12.71

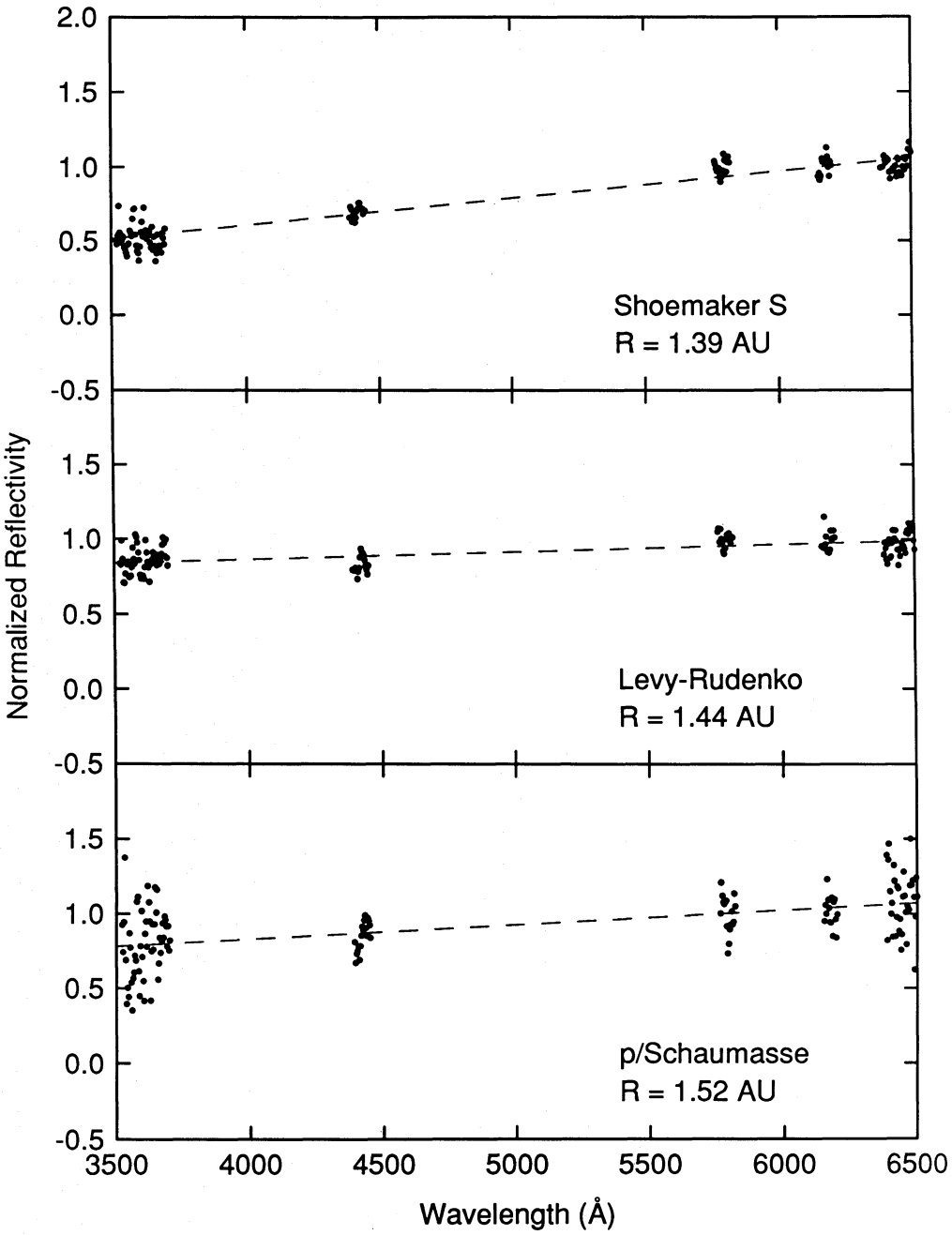

FIG. 2.—Optical reflectivities of the nine comets computed by dividing the spectra from Fig. 1 by the solar spectrum, as described in § III. The reflectivities are normalized to unity in the continuum interval $5760 < \lambda < 5820$ Å. Only those wavelengths observed to be free of molecular emission bands in all nine comets are plotted. *Dashed lines*, linear least-squares fits to the normalized reflectivities (see Tables 3 and 4). The comets are plotted at a fixed scale, except that the vertical axis of the plot for P/Gehrels 3 has twice the range of the other vertical axes.

CVF reflectivities of comets (resolution $\Delta\lambda \approx 0.05$ μm) compiled in Table 5 and shown in Figure 3. The plotted CVF measurements of comets P/Stephan-Oterma, Bowell, and Panther are reproduced from Jewitt *et al.* (1982), while the measurements of P/Swift-Gehrels and P/Wild 2 are from the present work. A CVF spectrum of P/Stephan-Oterma presented by A'Hearn, Dwek, and Tokunaga (1981) is similar to the one shown in Figure 3. The reflectivities have been systematically computed by dividing the measured flux densities by the solar flux density from Arvesen, Griffin, and Pearson (1969) and are normalized to unity at $\lambda = 2.2$ μm. The near-infrared reflectivities are seen to be approximately linear with wavelength, within the uncertainties of measurement; in this respect they resemble the optical reflectivities (Fig. 2). There are no sharp emission features which might be attributed to gas bands. Absorption features near $\lambda = 2.2$ μm in the spectra of comets Panther and Bowell (Jewitt *et al.* 1982), though significant, are not deep enough to show up clearly in the $J-H$ or $H-K$ colors. Values of $S'(\lambda_1, \lambda_2)$ calculated from the CVF data are similar to values found from the JHK photometry. In

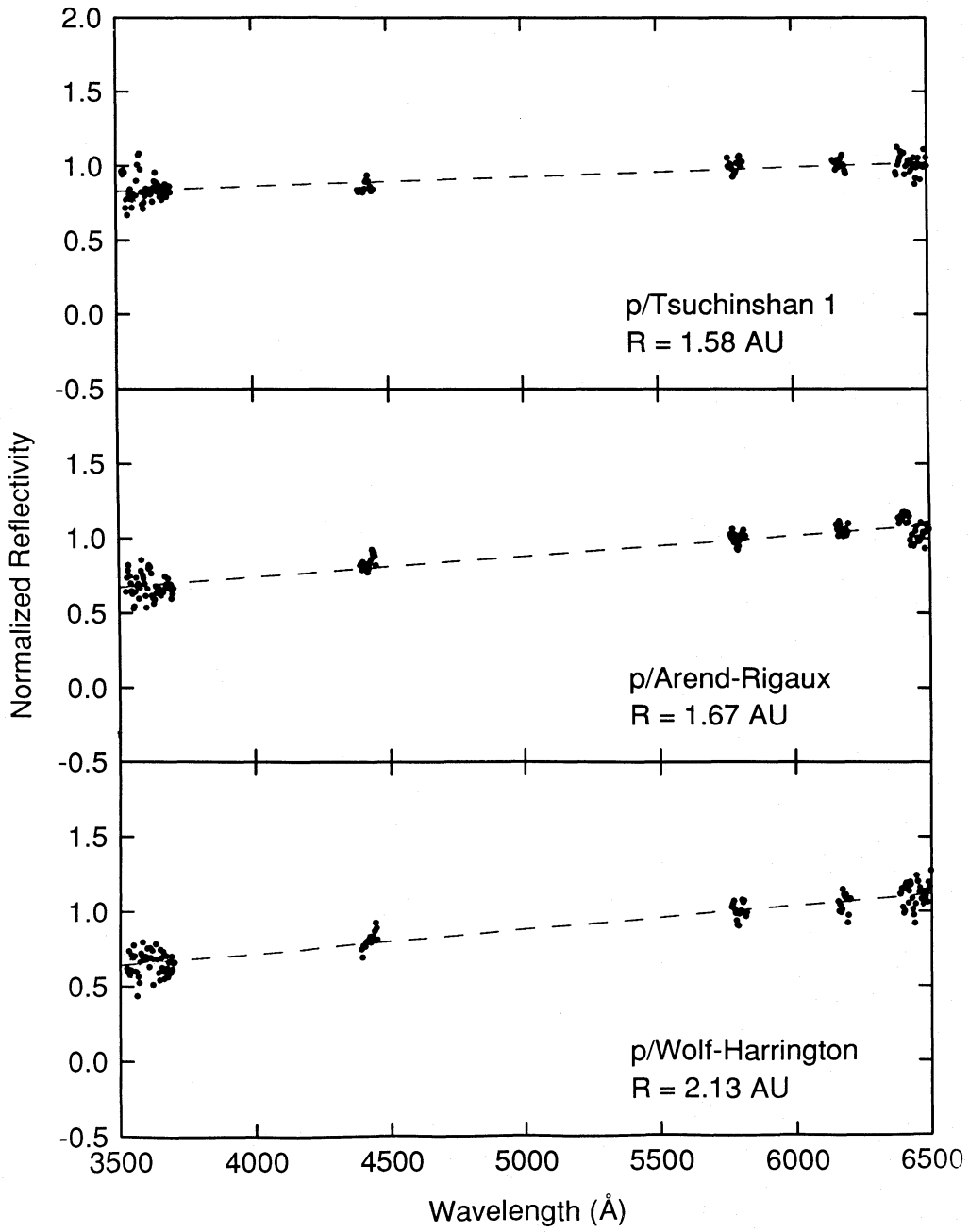

FIG. 2.—*Continued*

short, the existing CVF observations support the use of *JHK* filters to measure the gross wavelength dependence of the near-infrared scattering from cometary grains.

IV. DISCUSSION

a) Scattering as a Function of the Wavelength

The absolute reflectivities $S(\lambda)$ in the optical cannot be directly compared with those in the near-infrared since the measurements pertain to different comets at different times. However, it *is* possible to compare, in a statistical sense, the continuum *colors* measured in each of the three wavelength ranges. The values of $S'(\lambda_1, \lambda_2)$ calculated from the optical spectra and from the near-infrared photometry (Tables 3 and 4) are plotted versus the wavelength of observation in Figure 4. Near-infrared photometry of comets P/Stephan-Oterma, P/Kearns-Kwee, P/Gunn, and Elias (Hanner *et al.* 1984), comet Cernis (Hanner 1984), and comet Bowell (Hanner and Veeder 1984) has been included in Figure 4. We may disregard possible systematic effects between the Hanner *et al.* photometry and our photometry since we used the same telescope, detector, and filters and reduced all observations with reference to the same set of standard stars (Elias *et al.* 1982). Repeated, nearly simultaneous measurements of individual comets have been averaged to a single value before plotting to avoid giving undue weight to the more frequently observed (usually brighter) comets. A measurement of P/Grigg-Sjkellerup at $R = 1$ AU (Hanner *et al.* 1984) has been omitted from our

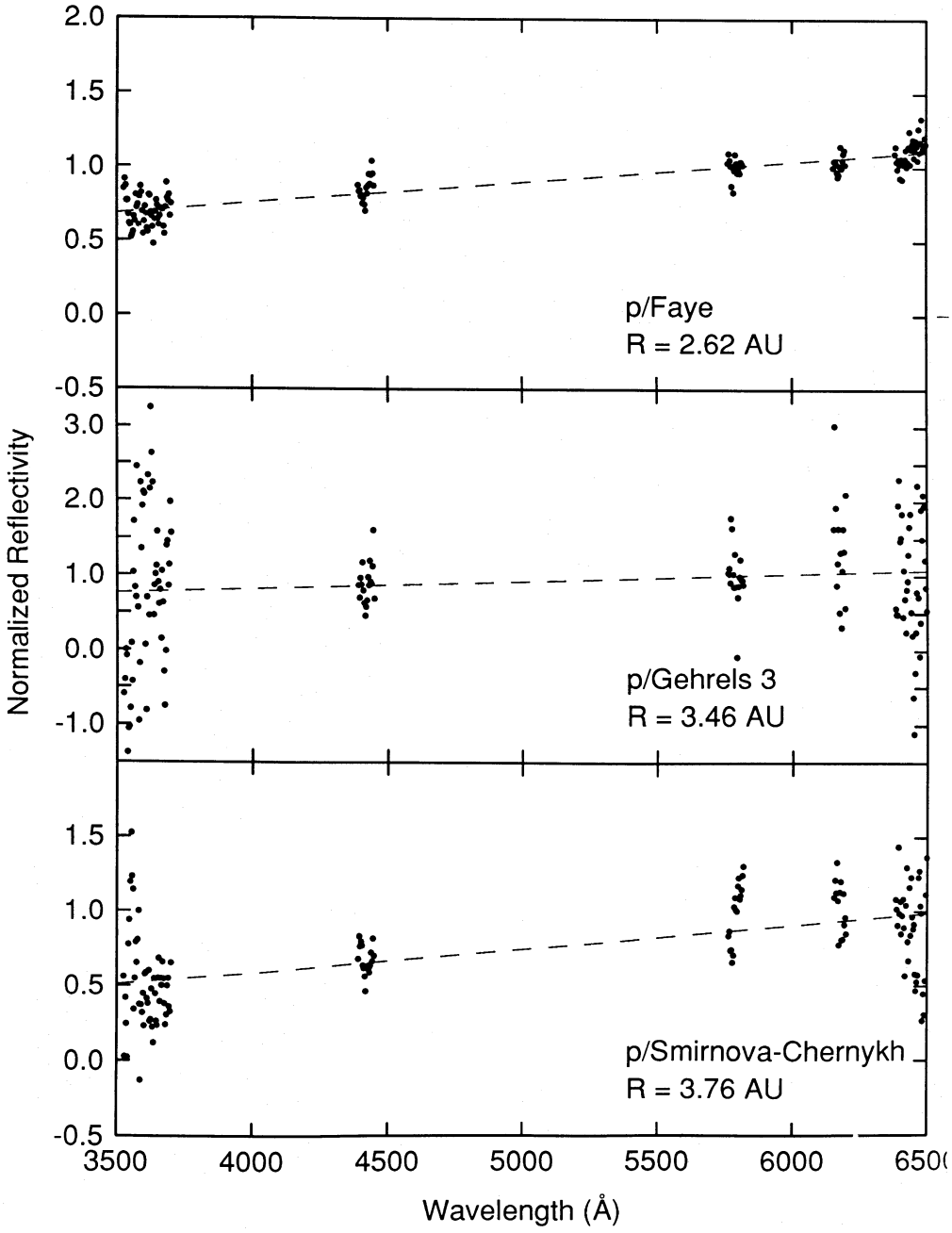

FIG. 2.—*Continued*

study because of the likelihood of thermal contamination of the K magnitude.

Qualitatively, Figure 4 shows that the continuum color changes progressively from red to neutral as the wavelength increases from the optical into the near-infrared. Solid circles with error bars represent the mean and the standard error on the mean of the observations within each of the observed wavelength regions. The average $S'(\lambda_1, \lambda_2)$ decreases systematically with increasing wavelength:

$$S'(0.35, 0.65) = (13 \pm 5)\% \text{ per } 10^3 \text{ Å} \quad (n = 9)\,,$$
$$S'(1.25, 1.65) = (3.2 \pm 1.6)\% \text{ per } 10^3 \text{ Å} \quad (n = 19)\,, \qquad (4)$$
$$S'(1.65, 2.20) = (0.5 \pm 1.3)\% \text{ per } 10^3 \text{ Å} \quad (n = 18)\,.$$

The mean normalized reflectivity gradient in the optical is consistent with the determinations by Stokes (1972), Remillard and Jewitt [1985; $S'(0.37, 0.73) = (11 \pm 3)\%$ per 10^3 Å from $n = 4$ comets], and Newburn and Spinrad [1985; $S'(0.47, 0.69) = (7 \pm 1)\%$ per 10^3 Å from $n = 17$ comets].

We obtained little photometry at wavelengths greater than 2.2 μm: most such photometry would in any case be contaminated by thermal emission from the grains. However, in the literature we find three determinations of the $K-L$ (2.2–3.5 μm) color in comets very far from the Sun. Specifically, A'Hearn, Dwek, and Tokunaga (1984) report $K-L$ colors -0.18, -0.35, and less than -0.42 mag in comets P/Gunn ($R = 2.77$ AU), Bowell 1980*b* ($R = 3.39$ AU), and Elias 1981c ($R = 5.13$ AU) respectively. Combined with the solar color

TABLE 5

CIRCULAR VARIABLE FILTER REFLECTIVITIES

A. PREVIOUS DATA

λ	P/Stephan-Oterma[a]	Bowell[a]	Panther[a]	P/Swift-Gehrels[b]
1.46...	...	0.88 ± 0.07	...	0.73 ± 0.05
1.50...	0.84 ± 0.11	0.94 ± 0.04	0.91 ± 0.02	0.75 ± 0.03
1.54...	0.83 ± 0.07	0.92 ± 0.03	0.89 ± 0.02	0.75 ± 0.03
1.58...	0.93 ± 0.08	0.94 ± 0.04	0.89 ± 0.02	0.77 ± 0.03
1.62...	0.85 ± 0.07	0.97 ± 0.03	0.88 ± 0.03	0.81 ± 0.03
1.66...	0.81 ± 0.05	0.87 ± 0.03	0.86 ± 0.02	0.71 ± 0.03
1.70...	0.87 ± 0.06	0.95 ± 0.03	0.88 ± 0.02	0.75 ± 0.03
1.74...	0.87 ± 0.06	0.94 ± 0.03	0.96 ± 0.02	0.83 ± 0.04
1.78...	1.02 ± 0.07	1.02 ± 0.05	1.09 ± 0.02	0.85 ± 0.04
2.00...	0.88 ± 0.06	0.90 ± 0.03	0.91 ± 0.02	0.91 ± 0.04
2.05...	0.91 ± 0.06	0.98 ± 0.03	0.96 ± 0.02	0.93 ± 0.04
2.10...	1.01 ± 0.07	1.03 ± 0.03	0.99 ± 0.02	0.95 ± 0.04
2.15...	0.95 ± 0.07	1.10 ± 0.04	1.10 ± 0.02	1.06 ± 0.06
2.20...	1.00	1.00	1.00	1.00
2.25...	1.17 ± 0.08	1.00 ± 0.04	0.99 ± 0.02	1.01 ± 0.04
2.30...	1.08 ± 0.10	1.03 ± 0.05	1.06 ± 0.02	1.02 ± 0.06
2.35...	1.03 ± 0.10	1.11 ± 0.05	1.17 ± 0.02	1.08 ± 0.07
2.40...	1.12 ± 0.09	1.21 ± 0.05	1.21 ± 0.02	1.12 ± 0.10
2.45...	...	1.25 ± 0.13	...	1.33 ± 0.13

B. THIS WORK

λ	P/Wild 2
1.38.....	0.75 ± 0.12
1.43.....	0.75 ± 0.08
1.48.....	0.81 ± 0.07
1.52.....	0.86 ± 0.08
1.62.....	0.97 ± 0.08
1.67.....	0.86 ± 0.08
1.72.....	0.86 ± 0.08
1.82.....	0.91 ± 0.08
2.00.....	1.02 ± 0.09
2.05.....	1.03 ± 0.09
2.11.....	0.91 ± 0.09
2.17.....	0.91 ± 0.09
2.22.....	1.08 ± 0.08
2.28.....	0.81 ± 0.07

[a] Jewitt *et al.* 1982.
[b] Neugebauer 1983.

$(K-L)_0 = 0.03$ and equation (3), the measurements yield normalized reflectivity gradients $S'(2.2, 3.5) = -1.5, -2.7$, and less than -3.1% per 10^3 Å respectively and the mean value

$$S'(2.20, 3.50) < (-2.4 \pm 0.7)\% \text{ per } 10^3 \text{ Å} \quad (n = 3) . \quad (5)$$

These results are included in Figure 4, where they are seen to continue the color-wavelength trend suggested by the observations at shorter wavelengths. A decrease in the reflectivity with increasing wavelength was commented on by A'Hearn, Dwek, and Tokunaga (1984). The trend in equations (4) and (5) is consistent with the CVF spectra of five comets (Fig. 3), within the uncertainties of the CVF data.

Continuum observations in the ultraviolet are especially difficult, as they are susceptible to the effects of strong UV emission lines. However, initial UV observations of five comets indicate reddened continua with $S'(0.26, 0.31) \approx 45\%$ per 10^3 Å (Feldman and A'Hearn 1985), apparently extending the trend for S' to increase with decreasing λ, as shown in Figure 4. Further observations in the ultraviolet with high spectral resolution and reliable instrumental calibration are highly desirable.

The observed color-wavelength relation (Fig. 4) has a possible interpretation in terms of the scattering from nonopaque homogeneous spheres (Van de Hulst 1957). The scattering efficiency Q_a of such particles depends on the ratio of the radius to the wavenumber, $X = 2\pi a/\lambda$, and on the complex refractive index, $n = n_r + in_i$. The phase shift between rays which pass centrally through the sphere and rays which graze the sphere at a tangent is $\Delta\phi = 2X(n_r - 1)$. Constructive interference of the central and tangential rays occurs when $\Delta\phi = 2\pi m$ ($m = 1, 2, 3, \ldots$). The first, and largest, maximum in the scattering efficiency, hence, occurs near $X_{\max} = \pi/(n_r - 1)$. Grains small compared to a wavelength have $X \ll X_{\max}$ and satisfy the Rayleigh approximation $Q_s = kX^4 \propto \lambda^{-4}$, so that the scattered radiation is relatively blue. For larger grains satisfying $X > X_{\max}$, the scattering efficiency falls from the maximum asymptotically toward the large-particle limit ($Q_s = 1$), and scattered radiation in this regime is relatively red. The neutral scattering observed near $\lambda \approx 2$ μm in comets would result if the grains satisfied $X \approx X_{\max}$, or equivalently, $a \approx \lambda/(2n_r - 2)$. For glassy terrestrial rocks, we may take $n_r = 3/2$ (Pollack, Toon, and Khare 1973), so that $X_{\max} \approx 2\pi \approx 6$ and $a \approx \lambda$. Therefore, the approximate particle radius $a \approx 2$ μm would give a wavelength dependence of the scattering similar to what is observed. Scattering at wavelengths $\lambda < 2$ μm would correspond to the $X > X_{\max}$ regime and could qualitatively account for the reddened optical continua. Scattering at wavelengths $\lambda > 2$ μm (corresponding to $X < X_{\max}$) would produce blue continua, as suggested by the available $K-L$ measurements.

This qualitative interpretation of the wavelength dependence of cometary scattering suggests an effective grain radius on the order of a few μm (depending on refractive index). It is interesting to note that similar estimates of grain size are obtained from independent methods. For instance, the trajectories of grains moving under the influence of solar radiation pressure indicate sizes of a few microns and larger (Finson and Probstein 1968; Sekanina and Miller 1973; Jambor 1973). The magnitude of the superheat observed in cometary grains is best explained by the small thermal infrared emissivities of micron-sized grains (Ney 1982). The phase function of the grains measured in one comet by Ney and Merrill (1976) is similar to the function calculated for micron-sized dielectric spheres. The large optical polarizations measured in some comets may be explained by scattering from grains of micron size (e.g., Myers and Nordsieck 1984), although other interpretations are possible. Recently, micron-sized grains were detected in the coma of P/Giacobini-Zinner by the *ICE* spacecraft (Gurnett *et al.* 1986).

However, our simple interpretation of the scattering neglects the effects of the distribution of sizes almost certainly present in every cometary coma. Also, no reference is made to the expected angle dependence of the scattered radiation, nor to the wavelength dependence of the complex refractive index. These defects could be corrected by a more detailed model of the scattering (if the compositions were known), but another, more troublesome problem must be faced. The scattering properties depend not only on the size and refractive index of the grains, and on the wavelength, but also on the grain shape. Interplanetary particles, probably derived from comets, may be collected in the stratosphere. The grains are roughly equidimensional but have complicated, re-entrant morphologies; some are reminiscent of bunches of grapes (Brownlee *et al.* 1976). In view of this, it does not seem likely that the Mie theory for scattering from homogeneous spherical particles will accurately reproduce the scattering properties of the real com-

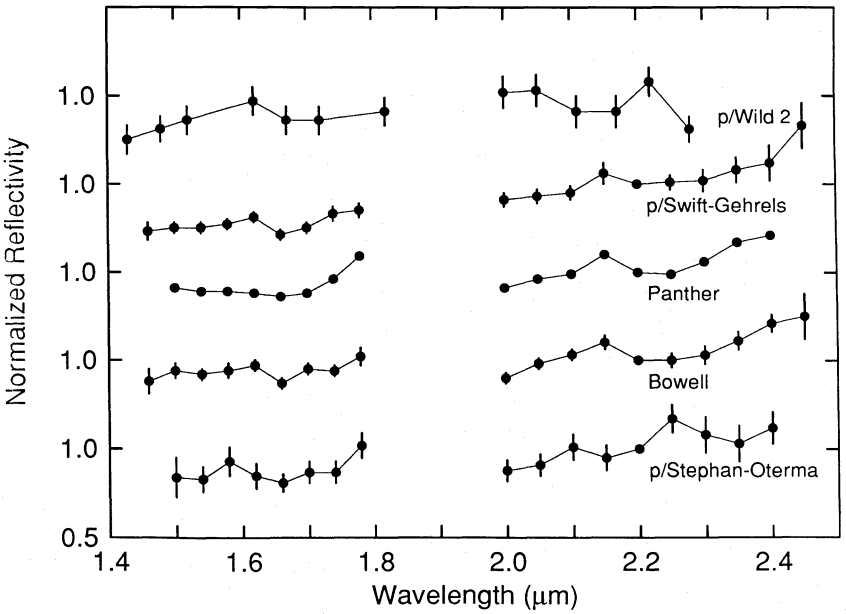

FIG. 3.—Near-infrared CVF reflectivities of comets, computed according to a standard procedure and normalized to unity at $\lambda = 2.2$ μm. Error bars are shown when the uncertainties of measurement exceed the radius of the black dots used to plot the data. The gap in the data near $\lambda = 1.9$ μm is due to atmospheric water opacity. Data for comets P/Stephan-Oterma, Panther, and Bowell are from Jewitt *et al.* (1982).

etary grains. This is especially true since comets are mostly observed in backscatter, where shape-dependent departures from ideal Mie behavior are particularly dramatic. Our calculations made using the Mie theory should therefore be taken to provide, at best, a crude representation of the scattering from cometary grains.

b) *Mie Scattering Calculations*

The Mie theory was used to compute the intensity of radiation scattered from a distribution of spherical, homogeneous particles having a range of complex refractive indices. Power-law size distributions were used, in which the number of grains having radii in the range a to $a + da$ is

$$n(a)da = Ka^{-m}da\,, \tag{6}$$

where K and m are constants for a given distribution. The intensity was calculated from

$$I_\lambda(\alpha) = \int I_\lambda(a, \alpha)n(a)da\,. \tag{7}$$

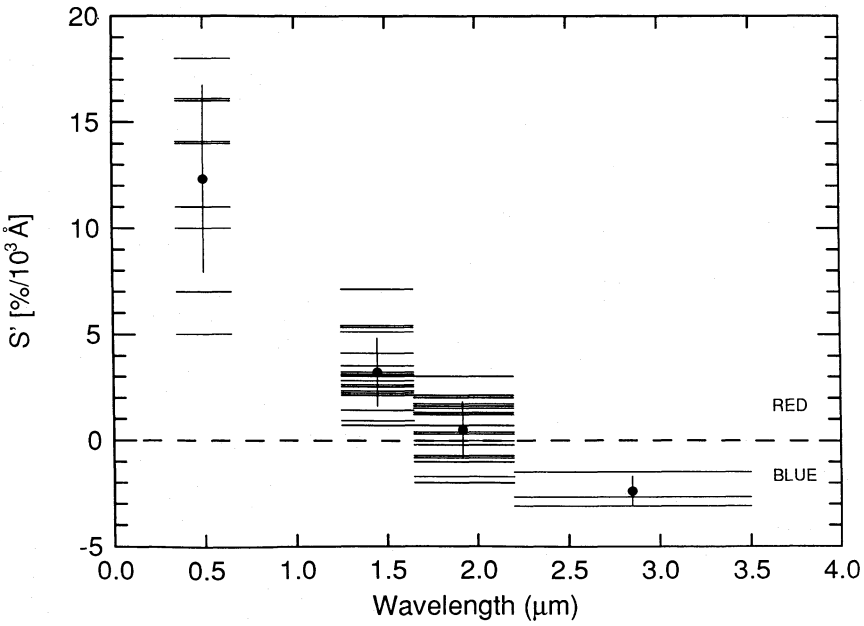

FIG. 4.—Normalized reflectivity gradient $S'(\lambda_1, \lambda_2)$ measured in percent per 10^3 Å, as a function of the wavelength of observation λ (μm). The plotted data are from Tables 3 and 5. Each comet is represented by a horizontal bar connecting the endpoint wavelengths λ_1 and λ_2. Neutral scattering is indicated by the dashed line at $S'(\lambda_1, \lambda_2) = 0$. Reddening of the scattered radiation is indicated by $S' > 0$, while enhanced blue scattering is indicated by $S' < 0$. The mean S' within each measured wavelength interval is plotted with a filled circle, and the 1 σ standard deviation on the mean is shown with a vertical line. The Figure shows that the color of the scattered radiation varies systematically with the wavelength of observation.

Here, $I_\lambda(a, \alpha)$ is the monochromatic scattered intensity from one particle of radius a, at phase angle α, computed from Mie theory. The integration extends over all particles in the range $a_{min} \leq a \leq a_{max}$. For each distribution, we computed the cross section weighted mean particle size

$$a_{mean} = \int a\pi a^2 n(a)da \Big/ \int \pi a^2 n(a)da \, . \quad (8)$$

A wide range of material refractive indices and grain size distributions gave continuum spectra compatible with the observed cometary continua. Calculations were made for materials having real refractive indices $1.3 < n_r < 1.9$ and imaginary indices $0 < n_i < 1$. The indices were taken to be constant with wavelength. The particle size limits used in each integration were allowed to vary within a wide range. For indices $m < 2.5$, the results were insensitive to the choice of the lower radius limit a_{min}, while for steeper distributions the results were insensitive to the upper limit a_{max}, provided $a_{max} \gg a_{min}$. The flat distributions (small m) generally matched the reddening of the cometary grains at small wavelengths, provided $a_{max} > 0.5$ μm. However, the flat distributions did not easily reproduce the color-wavelength trend seen in Figure 4, in the sense that the blue overturn at long wavelengths was not produced. We interpret this to mean that the flat distributions do not have enough grains satisfying $X \ll 1$ to produce Rayleigh scattering.

The grain size distributions determined from dynamical analyses of type II tails have $m \approx 4.4$ (Finson and Probstein 1968; Sekanina and Miller 1973; Jambor 1973) in the grain radius range $1 < a < 10$ μm. Thus, the mean dynamical radius (eq. [8]) is $a_{mean} = 2.2$ μm, very near the radius deduced from the wavelength dependence of the scattering on the basis of the qualitative argument in § IV*a*. The scattered intensity from an $m = 4.4$ distribution of slightly absorbing dielectric spheres with $a_{min} = 1$ μm is consistent with the observed reddening (the lower limit to the grain radius is $a_{min} \approx 0.2$ μm if the particles are strongly absorbent). Similar results were obtained for distribution indices $3.5 \leq m \leq 5.5$, except that steeper distributions tended to give blue scattering unless a_{min} was arbitrarily increased. Distributions with $a_{min} \ll 1$ μm in general give too much weight to small grains to match the reddened optical and near-IR scattering. This result is consistent with, but does not prove, the existence of a real deficiency of submicron grains in comets, as discussed by O'Dell (1974).

At the other extreme, it could be argued that the decrease in S' with increasing λ results not from geometric effects in the scattering from isolated small particles but from scattering in the rough surfaces of macroscopic ($a \gg \lambda$) particles. This would account for the qualitative similarity between the broad-band colors of the comets and the colors of many asteroids and meteorites (e.g., Johnson *et al.* 1975). This interpretation, although difficult to reconcile with the small grain sizes deduced from radiation pressure and other considerations (see § IV*a*) is by no means incompatible with the present measurements of the scattered radiation. Significantly, this radically different interpretation of the data would not change our conclusion that the optically important grains in comets are large compared to a wavelength.

c) Differences among the Grain Populations of the Comets

The scatter among the $S'(\lambda_1, \lambda_2)$ in each of the observed wavelength intervals in Figure 4 is large compared to the typical $\pm 2\%$ per 1000 Å uncertainties. Therefore, the scatter must be a result of real color differences among the comets. It is of interest to ask whether the color differences might be correlated with the observing geometry or some other quantity. For instance, it seems plausible that the mean grain size, and therefore the color, might change as the gas/dust momentum coupling decreases with increasing R. A difference might also be expected if the grains in distant comets retain ice while those closer to the Sun do not.

The normalized reflectivity gradients $S'(0.35, 0.65)$, $S'(1.25, 1.65)$, and $S'(1.65, 2.20)$ are plotted versus the heliocentric distance R (AU) in Figure 5. The correlation coefficients in each interval are listed in Table 6, together with the probability that an equal or larger correlation coefficient could be found in random, uncorrelated data. Neither $S'(0.35, 0.65)$, $S'(1.25, 1.65)$, nor $S'(1.65, 2.20)$ are significantly correlated with R. We conclude that there is no compelling evidence for a relation between the continuum colors of the comets and the heliocentric distance.

The absence of a correlation between the $S'(\lambda_1, \lambda_2)$ and the heliocentric distance implies that intrinsic color differences among the comets are large compared to any differences due to changing heliocentric distance. Likewise, there is no significant correlation between $S'(\lambda_1, \lambda_2)$ and the phase angle (Table 6). This confirms the result found by Remillard and Jewitt (1985) and Newburn and Spinrad (1985) and is consistent with the small color variations predicted in the observed phase angle range from scattering models (e.g., Campins and Hanner 1982). A contradictory finding was reported by Hartmann and Cruikshank (1984), who compared $J-H$ and $H-K$ observations of 14 comets in the heliocentric distance range $1 < R < 6$ AU and found the close comets to be red compared to the distant comets. In size, their data set is similar to the sets presented here (Tables 3 and 4). The main difference between their study and ours is that we have used near-infrared observations taken with a single telescope and detector and reduced using a single photometric system, whereas they have mixed photometry from several sources. Whether or not internal systematic errors are the reason for the difference of conclusions will best be judged from future systematic measurements of the near infrared colors of comets.

TABLE 6

CORRELATION COEFFICIENTS

Reflectivity Gradient[a]	Variable[b]	r_{AB}[c]	N[d]	$P(r > r_{AB})$[e]
$S'(0.35–0.65)$.....	R	+0.30	9	0.44
$S'(1.25–1.65)$.....	R	−0.36	19	0.12
$S'(1.65–2.20)$.....	R	−0.30	18	0.22
$S'(0.35–0.65)$.....	α	−0.23	9	0.57
$S'(1.25–1.65)$.....	α	+0.47	19	0.04
$S'(1.65–2.20)$.....	α	+0.25	18	0.31
$S'(0.35–0.65)$.....	$m(1, 1, 0)$	−0.43	9	0.25
$S'(1.25–1.65)$.....	$J(1, 1, 0)$	+0.33	19	0.17
$S'(1.65–2.20)$.....	$J(1, 1, 0)$	−0.05	18	0.82

[a] Normalized reflectivity gradient in wavelength range λ_1 to λ_2 microns.

[b] Variable with which a correlation is sought: R, heliocentric distance; α, phase angle; $m(1, 1, 0)$ and $J(1, 1, 0)$, geometrically corrected magnitudes (§ IV*c*).

[c] Linear correlation coefficient.

[d] Number of data pairs in the correlation calculation.

[e] Probability that a correlation larger than the calculated one could be obtained from a random, uncorrelated parent population. Generally, $P > 0.01$ indicates that the correlation is insignificant, while $P < 0.01$ indicates that a significant correlation may exist.

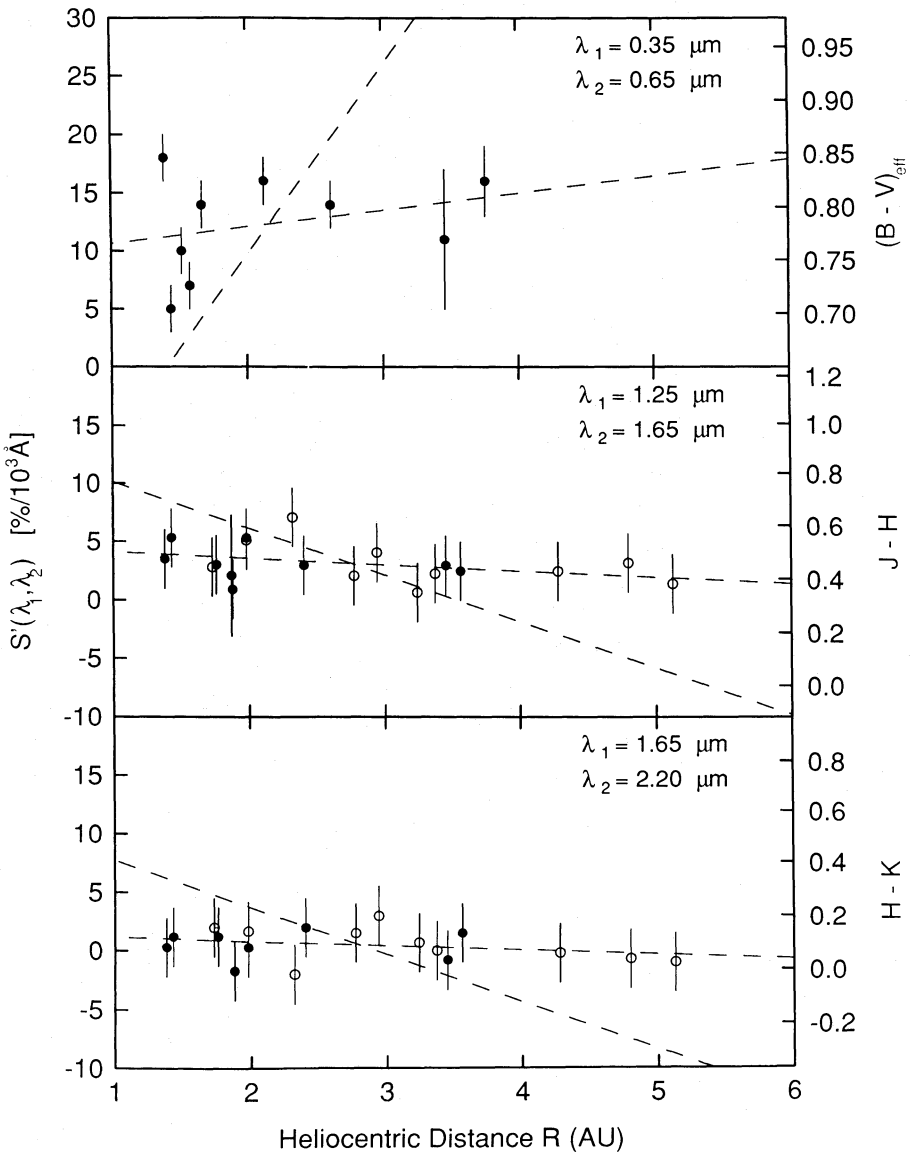

FIG. 5.—Normalized reflectivity gradient $S'(\lambda_1, \lambda_2)$ vs. heliocentric distance R (AU) for each of the observed wavelength ranges. $S'(\lambda_1, \lambda_2) = 0$ indicates neutral scattering. *Filled circles*, present work; *open circles*, other sources (see Table 3). Dashed lines are from a linear regression analysis (see Table 6). The $B-V$, $J-H$, and $H-K$ colors are indicated on the right-hand side of the figure. The effective $B-V$ colors are obtained from eq. (3), assuming $(B-V)_{\odot} = 0.65$.

To test for a possible correlation of S' with the total grain cross section, we have used F_λ, the flux density in the $5760 \leq \lambda \leq 5820$ Å continuum window, to compute the continuum magnitude

$$m_{5790} = -2.5 \log (F_\lambda) - 28.58 . \quad (9)$$

The constant in equation (9) is such that m_{5790} would exactly equal the apparent V-magnitude of the continuum if the cometary spectrum were flat; for practical purposes m_{5790} and V can be considered the same. The magnitude of the continuum within the projected spectrometer diaphragm, reduced to $R = \Delta = 1$ AU and $\alpha = 0$, was computed from

$$m(1, 1, 0) = m_{5790} - 2.5 \log (R^2\Delta) - \phi\alpha . \quad (10)$$

The phase coefficient was taken to be $\phi = 0.04$ mag per degree. The values of m_{5790} and $m(1, 1, 0)$ are listed for each comet in Table 4. Similarly, the geometrically corrected infrared magnitude $J(1, 1, 0)$ is tabulated for each comet in Table 3. The geometrically corrected magnitudes $m(1, 1, 0)$ and $J(1, 1, 0)$ are direct measures of the product of the geometric albedo of the grains with the total grain cross section. Table 6 summarizes the results of correlation tests performed on S' versus $m(1, 1, 0)$ and on S' versus $J(1, 1, 0)$. No significant correlations are apparent. The CN band at 3880 Å was used to estimate the gas production rate in each comet according to the procedure used by Remillard and Jewitt (1985). No compelling correlation of $S'(0.35, 0.65)$ with the CN column density, the CN production rate, or the apparent gas/dust ratio within the spectrometer diaphragm was found. A detailed analysis of the gas components of these and other comets will be presented in a later paper.

To test whether the continuum color might be correlated with the dynamical ages or irradiation histories of the comets, we have separately computed the mean $S'(\lambda_1, \lambda_2)$ in the $J-H$

and $H-K$ wavelength intervals for the long-period comets (specifically Cernis, Bowell, and Elias) and the short-period comets (all others in Table 3). Any difference between the mean colors of the long- and short-period comets is small compared to the standard errors on these means, so that no evidence for an irradiation age versus color relation can be claimed. A correlation of this sort might be expected if the grain properties vary with depth in the nucleus, perhaps as a result of cosmic-ray irradiation of the outer layers of the nucleus. Our conclusion is tentative, in view of the preponderance of short-period comets over long-period ones in our observational sample.

The lack of significant correlations in Table 6 suggests that the grain populations in different comets are *intrinsically* different. This conclusion is supported by an examination of cometary superheat measurements (e.g., Ney 1982). The superheat, which depends on the ratio of the grain emissivities at thermal and optical wavelengths, shows a wide range of values at a given R. Small differences in the grain size distribution or in the grain composition could cause color, and superheat, differences of the magnitudes observed. For instance, changing the mean grain size by a factor of order 2 could account for the observed range of superheats. Finding how or even whether differences in the grain properties are related to differences in the formation conditions of the comets is an intriguing topic for further research.

d) Comparison with Interstellar Grains

A comparison between cometary grains and their interstellar counterparts is surprisingly difficult. This difficulty arises because cometary grains are studied using scattered and thermally emitted radiation, whereas interstellar grains are best known from their effects on the *extinction* of starlight. Essentially nothing is known about the extinction properties of cometary grains, and relatively little is known about the scattering properties of interstellar grains; thus we find little common ground on which to base a comparison between the two types of particle.

The most important optical property of the interstellar grains is their $1/\lambda$ extinction law, which holds from ultraviolet to infrared wavelengths. This form of extinction is consistent with a prevalence of small grains ($a < \lambda$) in the interstellar medium. The derived grain size is model-dependent, but most models suggest a mean particle radius $a_{\rm mean} \approx 0.2$ μm. The wavelength dependence of the extinction in the range $0.35 < \lambda < 2.20$ μm is rather featureless and does not by itself provide a very strong constraint on the composition of the grains. A strong compositional clue is provided by a broad interstellar extinction enhancement at $\lambda \approx 0.22$ μm. This feature is often attributed to graphite, but carbon structures which are less ordered than graphite may also explain the feature and may be easier to form in the atmospheres of carbon stars (Sakata *et al.* 1983). Pregraphitic particles, or PAHs (polycyclic aromatic hydrocarbons) with molecular weights of a few hundred or more, may be ubiquitous in interstellar space and may produce the 0.22 μm feature. Other compositional constraints include a feature near $\lambda \approx 10$ μm (normally attributed to a vibrational transition in amorphous silicates) and several emission features in the 3–12 μm region (possibly due to vibrations in large aromatic hydrocarbon solids, see Sakata *et al.* 1984; Cohen, Tielens, and Allamandola 1985). The 10 μm feature is seen in some comets (e.g., Ney 1982), but we know of no observations of the 0.22 μm absorption or the near-infrared emission features in comets.

Composite models of the interstellar extinction and polarization by Mathis, Rumpl, and Nordsieck (1977) lead to power-law grain size distributions with index $3.3 < m < 3.6$, and with radius limits $a_{\rm min} \approx 0.005$ μm and $a_{\rm max} \approx 1$ μm (depending on the assumed composition). Roughly equal numbers of graphite (their assumed 0.22 μm carrier) and silicate grains were needed to match the 0.22 μm interstellar feature and the general extinction. Mie calculations of the scattering expected from the Mathis *et al.* interstellar distribution produce relatively blue continua and hence suggest that this distribution does not accurately describe the cometary grains. (In this regard, it is worth noting that, at optical wavelengths, many reflection nebulae are blue with respect to their illuminating stars. However, the interpretation of reflection nebulae is complicated since these objects, unlike comets, tend to be optically thick. Multiple scattering is important, and the scattered intensity is a function of the [typically unknown] geometry of the dust cloud as well as of the grain properties.) The Mathis *et al.* distribution *can* be made to fit the reddened cometary continua if the small (blue) particles are artificially removed by increasing the lower size limit to $a_{\rm min} \approx 1$ μm ($a_{\rm max}$ can be increased to an arbitrarily large value since the distribution is steep). Thus, it again appears that the optically weighted mean grain size in comets is about an order of magnitude larger than the size of the grains in the interstellar medium. Grains of submicron size are certainly present in comets, but they do not dominate the optical cross section as they do in the interstellar medium.

There is evidence that the grains in some molecular clouds are larger than the grains in the open interstellar medium (e.g., Castellaz *et al.* 1985), suggesting the occurrence of grain growth in these clouds. The still larger mean size of the cometary grains is probably a result of grain growth in the nebula from which the comets, and the solar system, condensed. Unfortunately, the present scattering observations throw no light on the question of whether the cometary grains grew by the accretion of monomers from a condensing hot solar nebula or by the cold agglomeration of pre-existing interstellar grains under the influence of contact forces. This question is relevant because we would like to know whether the comet grains have been heated and chemically changed during the formation of the solar system or whether they contain unaltered interstellar material. Anomalous oxygen isotopic ratios in some *meteorites* (Clayton 1981) may attest to the survival of limited amounts of interstellar material in the solar system. Thus it is at least plausible that cometary grains might contain unaltered interstellar matter (see also Greenberg 1982).

We find it interesting to consider the hypothesis that the larger mean size of the cometary grains, as compared to the interstellar grains, is a simple consequence of the depletion of small grains from an initial interstellar size distribution by agglomeration. Rapid grain growth is certainly to be expected in any nebula both cool and dense enough to form a cometary nucleus. The potential importance of agglomeration is suggested by the following calculation, in which agglomerated grains are shown to form even before hydrostatic equilibrium is attained by the solar nebula.

Substantial grain growth will occur if the time scale for the agglomeration τ_a is short compared to the free-fall collapse time for the nebula, $\tau_{\rm ff}$. The collision rate among grains of initial radius a_0 (m), in a gas where the density of interstellar grains is N_1 (m^{-3}), is of order C (s^{-1}) $= 4\pi a_0^2 N_1 \Delta v$. Here, Δv (m s^{-1}) is the velocity dispersion among the grains. The agglomeration time is of order $\tau_a \approx (fC)^{-1}$, where f is the frac-

tion of the collisions which result in sticking. Each interstellar grain has a mass m (kg) $= 4\pi\rho a_0^3/3$. The number density of interstellar grains is given by $N_1 = (\kappa\mu m_H/m)N_{gas}$, where N_{gas} (m^{-3}) is the total gas density, μ is the gas molecular weight, $m_H = 1.67 \times 10^{-27}$ kg is the mass of a hydrogen atom, and $\kappa \approx 6 \times 10^{-3}$ (Spitzer 1978) is the ratio of the mass of interstellar grains to the total gas mass within a fixed volume of interstellar space (we ignore the reduction of N_1 as a result of the depletion of the small grains in this simple treatment). Hence, we estimate the agglomeration time

$$\tau_a \approx \rho a_0/(3\kappa\mu m_H f N_{gas} \Delta v) . \quad (11)$$

The free-fall time for a cloud of initial density N_{gas} is $\tau_{ff} \approx [3\pi/(32G\mu m_H N_{gas})]^{1/2}$. Significant agglomeration is expected in any cloud for which $\tau_{ff} \gg \tau_a$, or

$$N_{gas} \gg [32G/(27\pi\mu m_H)][\rho a_0/(\kappa f \Delta v)]^2 . \quad (12)$$

The density and radius of the grains are taken to be $\rho = 2000$ kg m^{-3} and $a_0 = 10^{-7}$ m, and we take $\mu = 2$ as appropriate for a molecular hydrogen cloud. The grain velocity dispersion Δv will likely be determined by the velocities of turbulent cells in the collapsing cloud and is thus rather poorly known. A practical *upper* limit to Δv may be set by estimating the velocity at which colliding grains would fracture. For bond strengths $E \approx 1$ eV, bond lengths $b \approx 3 \times 10^{-10}$ m and $a_0 = 10^{-7}$ m, this velocity is $\Delta v \approx (\rho b^2 a_0/E)^{-1/2} \approx 100$ m s^{-1}. The ultimate *lower* limit, $\Delta v \approx 10^{-2}$ m s^{-1}, is set by Brownian motion. However, a more plausible lower limit, $\Delta v \approx 1$ m s^{-1}, is set by the differential radiation pressure acceleration owing to young stars in and near the collapsing cloud. We adopt $1 < \Delta v < 100$ m s^{-1} to bracket the plausible range of grain collision speeds and to calculate the critical density from equation (12). For perfect sticking efficiency, $f = 1$, we find that agglomeration should occur in a free-fall time in any cloud with $N_{gas} \gg 1 \times 10^9$ m^{-3} (for $\Delta v = 100$ m s^{-1}) and with $N_{gas} \gg 1 \times 10^{13}$ m^{-3} (for $\Delta v = 1$ m s^{-1}). These modest densities are typical of clouds in the early and middle stages of collapse respectively, and our result is consistent with the detection of larger grains in molecular clouds as noted above. Densities in the solar nebula were still higher by many orders of magnitude. Thus, we infer that the cometary grains could have formed at low temperatures by agglomeration during free fall. Further growth by agglomeration would proceed rapidly in the high-density hydrostatic solar nebula produced by the collapse. These early agglomerates would probably escape vaporization in all but the innermost part of the solar nebula and could be incorporated in comets with little or no metamorphism. Thus, although there is a physical (size) difference between cometary and interstellar grains, this difference could have arisen by grain agglomeration at low temperatures and cannot be presumed to imply a chemical difference.

In this simplified view, the structural subunits of the "bunch of grapes" interplanetary particles (Brownlee *et al.* 1976) would be the individual, possibly unaltered, interstellar grains. The dimensions of the subunits, $a \approx 0.1$ μm (Fraundorf, Brownlee, and Walker 1982) are indeed similar to the dimensions of the dominant interstellar grains (Mathis, Rumpl, and Nordsieck 1977). Furthermore, the Mathis *et al.* power-law distributions are steeper than a^{-3}, so that they contain enough small particles to produce the $a \approx 1$ μm cometary grains by agglomeration. If the agglomeration hypothesis is correct, we must expect to find subunits of various compositions mixed within each cometary grain, corresponding to the different grain types in the interstellar medium. Such is the case in the interplanetary particles, in which grains of silicate composition are found mixed with a dark, carbon-rich matrix material (Bradley, Brownlee, and Fraundorf 1984). The bulk of the matrix consists of amorphous carbon, while large pieces of crystalline carbon (graphite) are rare. A complex carbonaceous composite material, which may be similar to the dark matrix, has been simulated in the laboratory by Sakata *et al.* (1983, 1984). The composite, which shows the 0.22 μm feature in absorption, consists of a complex mixture of small graphitic structures and conjugated double-bond hydrocarbons. This material is a potential carrier of the 0.22 μm interstellar feature. Detection of the 0.22 μm feature in the scattering from the carbon-rich matrix in interplanetary particles, or from comets directly, would provide strong evidence supporting the incorporation of interstellar material in comets. For now, we can only conclude that agglomeration provides a natural mechanism by which interstellar grains could have coalesced to cometary grain sizes and that this agglomeration hypothesis appears consistent with the basic properties of both cometary and interstellar grains. The possibility that interstellar grains may be available for study within the solar system clearly deserves rigorous investigation.

V. CONCLUSIONS

1. The normalized rate of change of the reflectivity of cometary grains with respect to the wavelength of observation decreases as the wavelength increases. The continuum color changes progressively from red to neutral as the wavelength increases from the optical ($\lambda \approx 0.5$ μm) into the near-infrared ($\lambda > 2$ μm).

2. The observed wavelength dependence of the reflectivity gradient is consistent with an origin by scattering from micron-sized or larger, slightly absorbing spheres. Power-law size distributions of grains having optically weighted mean grain radii $a \geq 1$ μm are also consistent with the reflectivity gradient versus wavelength relation. From the scattered radiation alone, we cannot exclude the possibility that the scatterers in comets are rough macroscopic surfaces ($a \gg \lambda$). Although optically small grains ($a < \lambda$) are undoubtedly present in the comae of the observed comets, the scattering cross section lies in particles which are optically large ($a > \lambda$).

3. The optically important comet grains are about an order of magnitude larger than the optically important interstellar grains. This size difference is a probable result of grain growth in the cloud from which the comets condensed. The hypothesis that the cometary grains are low-temperature agglomerates of interstellar particles is apparently consistent with the known properties of both cometary and interstellar grains.

4. Grain properties differ so widely among the comets that any phase angle or heliocentric distance dependences of the continuum color are hidden. The color differences, and related superheat differences, appear to be intrinsic to the comets and may be caused by small differences in the grain size distributions or in the grain compositions.

We thank Dave Griep, Charlie Kaminski (IRTF), and Randy Bergeron (KPNO) for efficient control of the telescopes. The Kitt Peak staff made a timely and much-needed modification to the 2.1 m guide-probe control software so that we

could take the IIDS observations described in this paper. We especially thank Jeannette Barnes for help with the downtown computer reduction. The optical spectra were analyzed on the MIT Planetary Astronomy VAX. This work was done in part using funds provided by the NASA Planetary Astronomy Program.

REFERENCES

A'Hearn, M. F. 1982, in *Comets*, ed. L. L. Wilkening (Tucson: University of Arizona Press), p. 433.
A'Hearn, M. F., Dwek, E., and Tokunaga, A. T. 1981, *Ap. J. (Letters)*, **248**, L147.
———. 1984, *Ap. J.*, **282**, 803.
Arvesen, J. C., Griffin, R. N., and Pearson, B. D. 1969, *Appl. Optics*, **8**, 2215.
Bradley, J. P., Brownlee, D. E., and Fraundorf, P. 1984, *Science*, **223**, 56.
Brownlee, D. E., Horz, F., Tomandl, D. A., and Hodge, P. W. 1976, in *The Study of Comets*, ed. B. Donn (NASA SP-393), p. 962.
Campins, H., and Hanner, M. S. 1982, in *Comets*, ed. L. L. Wilkening (Tucson: University of Arizona Press), p. 341.
Campins, H., Rieke, G. H., and Lebofsky, M. J. 1985, *A.J.*, **90**, 896.
Castellaz, M. W., Hackwell, J. A., Grasdalen, G. L., Gehrz, R. D., and Gullixson, C. 1985, *Ap. J.*, **290**, 261.
Clayton, R. N. 1981, *Phil. Trans. Roy. Soc. London, A*, **303**, 339.
Cohen, M., Tielens, A. G. G. M., and Allamandola, L. J. 1985, *Ap. J. (Letters)*, **299**, L93.
Elias, J. H., Frogel, J. A., Matthews, K., and Neugebauer, G. 1982, *A.J.*, **87**, 1029.
Feldman, P. D., and A'Hearn, M. F. 1985, in *Ices in the Solar System*, ed. J. Klinger, *et al.* (Dordrecht: Reidel), p. 453.
Finson, M. L., and Probstein, R. F. 1968, *Ap. J.*, **154**, 353.
Fraundorf, P., Brownlee, D. E., and Walker, R. M. 1982, in *Comets*, ed. L. L. Wilkening (Tucson: University of Arizona Press), p. 383.
Greenberg, J. M. 1982, in *Comets*, ed. L. L. Wilkening (Tucson: University of Arizona Press), p. 131.
Gurnett, D. A., Averkamp, T. F., Scarf, F. L., and Grun, E. 1986, *Geophys. Res. Letters*, **13**, 291.
Hanner, M. S. 1980, in *IAU Symposium 90, Solid Particles in the Solar System*, ed. I. Halliday and B. McIntosh, p. 223.
———. 1984, *Ap. J. (Letters)*, **277**, L75.
Hanner, M. S., Tokunaga, A. T., Veeder, G. J., and A'Hearn, M. F. 1984, *A.J.*, **89**, 162.
Hanner, M. S., and Veeder, G. J. 1984, *Icarus*, **60**, 445.
Hartmann, W. K., and Cruikshank, D. P. 1984, *Icarus*, **57**, 55.
Jambor, B. J. 1973, *Ap. J.*, **185**, 727.
Jewitt, D. C., Soifer, B. T., Neugebauer, G., Matthews, K., and Danielson, G. E. 1982, *A.J.*, **87**, 1854.
Johnson, T. V., Matson, D. L., Veeder, G. J., and Loer, S. J. 1975, *Ap. J.*, **197**, 527.
Mathis, J. S., Rumpl, W., and Nordsieck, K. H. 1977, *Ap. J.*, **217**, 425.
Myers, R. V., and Nordsieck, K. H. 1984, *Icarus*, **58**, 431.
Neugebauer, G. 1983, private communication.
Newburn, R. L., and Spinrad, H. 1985, *A.J.*, **90**, 2591.
Ney, E. P. 1982, in *Comets*, ed. L. L. Wilkening (Tucson: University of Arizona Press), p. 323.
Ney, E. P., and Merrill, K. M. 1976, *Science*, **194**, 1051.
O'Dell, C. R. 1974, *Icarus*, **21**, 96.
Oke, J. B. 1974, *Ap. J. Suppl.*, **27**, 21.
Pollack, J. B., Toon, O. B., and Khare, B. N. 1973, *Icarus*, **19**, 372.
Remillard, R. A., and Jewitt, D. C. 1985, *Icarus*, **64**, 27.
Sakata, A., Wada, S., Okutsu, Y., Shintani, H., and Nakada, Y. 1983, *Nature*, **301**, 493.
Sakata, A., Wada, S., Tanabe, T., and Onaka, T. 1984. *Ap. J. (Letters)*, **287**, L51.
Sekanina, Z., and Miller, F. D. 1973, *Science*, **179**, 565.
Spitzer, L. 1978, *Physical Processes in the Interstellar Medium* (New York: Wiley), p. 162.
Stokes, G. M. 1972, *Ap. J.*, **177**, 829.
Stone, R. P. S. 1977, *Ap. J.*, **218**, 767.
Van de Hulst, H. C. 1957, *Light Scattering by Small Particles* (New York: Wiley).

Note added in proof.—Subsequent to the acceptance of this paper for publication, *in situ* measurements of the dust particle properties in the coma of comet P/Halley have become available. Measurements from dust particle impact counters on the *Giotto* and *Vega* spacecraft suggest a differential grain size distribution index $m \approx -3$ (J. A. M. McDonnell *et al.*, *Nature*, **321**, 338 [1986]; J. A. Simpson *et al.*, *Nature*, **321**, 278 [1986]). The distribution extends at least to grain masses of $\sim 10^{-20}$ kg, corresponding to grain radii of order 10^{-8} m. Although the abundance of small grains is larger than expected, the cross section–weighted mean size (eq. [8]) of the grains in Halley is $a > 1$ μm, so that our inferences concerning particle size (see conclusion No. 2) are confirmed. In addition, we have measured the scattered continuum in P/Halley using the ground-based methods described in this paper. We find $S'(0.37, 0.70) \approx 10\%$ per 1000 Å, well within the range of values determined for other comets in Table 4.

D. C. Jewitt and K. J. Meech: 54-418, Department of Earth, Atmospheric and Planetary Sciences, Massachusetts Institute of Technology, Cambridge, MA 02139